International Immunopharmacology 73 (2019) 362–369

Contents lists available at ScienceDirect

International Immunopharmacology

journal homepage: www.elsevier.com/locate/intimp

The roles of synovial hyperplasia, angiogenesis and osteoclastogenesis in the protective effect of apigenin on collagen-induced arthritis

Yunxia Li[a,*], Biao Yang[b], Jia-yu Bai[a], Shuyue Xia[a], Mingqing Mao[a], Xiaoyang Li[a], Nan Li[a], Lei Chen[a]

[a] Department of Respiratory Medicine, Affiliated Center Hospital of Shenyang Medical College, Shenyang 110024, China
[b] Laboratory of Microbiology, School of Basic Medical Science, Shenyang Medical College, Shenyang 110024, China

ARTICLE INFO

Keywords:
Apigenin
Rheumatoid arthritis
Synovial hyperplasia
Angiogenesis
Osteoclastogenesis

ABSTRACT

Apigenin (API) is a plant flavone that is known to exert a protective effect in rheumatoid arthritis (RA), which is a chronic autoimmune disease. However, the molecular mechanism for API's protective effect against RA is still unclear. Here, a collagen-induced arthritis (CIA) mouse model was used to assess the protective effect of API on RA. Histomorphological studies, immunohistochemistry, RT-PCR, and western blot were conducted to elucidate the roles of synovial hyperplasia, angiogenesis, and osteoclastogenesis in the protective effect of API on RA. Fibroblast-like synoviocytes (FLSs) were isolated to measure the effect of API on FLS proliferation and apoptosis. API exhibited a significant protective effect in CIA mice in a dose- and time-dependent manner. An increase in apoptosis and decrease in proliferation were observed after the API treatment in FLSs, suggesting that API might inhibit synovial hyperplasia. Moreover, CIA angiogenesis was repressed by API via down-regulation of VEGF and VEGFR. Furthermore, API regulated the osteoclastogenesis-associated RANKL/RANK/OPG system in CIA mice. Therefore, API inhibits CIA by repressing synovial hyperplasia, angiogenesis, and osteoclastogenesis. This suggested that API might be a putative low toxicity candidate drug for RA treatment.

1. Introduction

Rheumatoid Arthritis (RA), a chronic autoimmune disease of unknown etiology, affects about 1% of the population worldwide. It is characterized by joint synovial inflammation and progressive cartilage and bone destruction, resulting in gradual immobility [1].

In RA, fibroblast-like synoviocytes (FLSs) can be recruited to the synovial intimal lining and contribute to the local production of cytokines, small molecule mediators of inflammation, and proteolytic enzymes that degrade the extracellular matrix [2]. The imbalance between FLS proliferation and apoptosis has been regarded as a contributing factor for the development of RA [3]. In addition, abundant blood vessels were observed in the RA synovium that are likely to be involved in the development of RA [4]. Furthermore, bone erosion starts early following the onset of RA and progresses throughout the course of the disease. As the primary bone resorptive cells, osteoclasts play an important role in bone destruction in RA [5]. Activation of the receptor activator in the nuclear factor κB ligand (RANKL) pathway increases osteoclast formation in the joints, thus promoting bone destruction in RA [6–8].

Non-steroidal anti-inflammatory drugs and disease-modifying antirheumatic drugs (DMARDs) have been clinically used for RA treatment. In particular, the use of DMARDs that act on the immune system significantly slows down the progression of RA. However, the potent synthetic drug treatments cause severe toxicity. For example, methotrexate, the first-line therapy for the treatment of RA, resulted in many adverse effects, including hepatotoxicity, ulcerative stomatitis, leukopenia, neurological damage, and memory loss during long-time treatment. Therefore, herbal drugs are gaining interest among RA patients due to their safety [9].

Apigenin (API, 4, 5, 7-trihydroxy flavone) is a plant flavone that exists in common fruits and vegetables, including parsley, celery, celeriac, and chamomile tea. It possesses strong anti-inflammatory and anticancer properties. Epidemiologic studies suggest that flavone-enriched diet is related to a decreased risk of certain cancers [10]. It has also been suggested that API may be protective in autoimmune diseases, such as lupus [11], asthma [12], and RA [13]. API treatment delayed the onset and reduced the severity of arthritis in collagen-induced arthritic (CIA) mice, diminished secretion of pro-inflammatory cytokines in the serum, and suppressed dendritic cell maturation and

* Corresponding author.
E-mail address: 782186096@qq.com (Y. Li).

https://doi.org/10.1016/j.intimp.2019.05.024
Received 5 April 2019; Received in revised form 7 May 2019; Accepted 11 May 2019
Available online 24 May 2019

Table 1
Primer sequences of qRT-PCR.

Name	Forward primer	Reverse primer
Tnfsf11	CATCGGGTTCCCATAAAG	GAAGCAAATGTTGGCGTA
Tnfrsf11a	CAAGGAGGCCCAGGTTTA	CAGATTAGCTGTCAGCGTTTT
Tnfrsf11b	CATACCACTTTCCCAAAACCGTC	TCAACTGCCATTTCAAGAGCC
Vegf	CTGACGGACAGACAGACAGACAC	GCCCAGAAGTTGGACGAAAA
Vegfr-1	CGGAGAAATCTGCTCGCTAT	CTTGGAAGGGACGACACG
Vegfr-2	TAACTATCCGAAGGGTGA	AAGGAGCCAGAAGAACAT
Actb	GGAGATTACTGCCCTGGCTCCTAGC	GGCCGGACTCATCGTACTCCTGCTT

migration [13]. However, this mechanism is still not well-understood. We sought to analyze the effect of API on synovial hyperplasia, angiogenesis, and osteoclastogenesis in a CIA mouse model. This work aimed to clarify the mechanism of API on RA treatment.

2. Materials and methods

2.1. Mice

DBA/1J male mice (6–8 weeks, 22.5 ± 2.5 g), which were purchased from Beijing Huafukang bioscience CO, were used. Experiments were performed in accordance with the guidelines of the Animal Care and Use Committee of Shenyang Medical College.

2.2. Collagen-induced arthritis model and apigenin treatment

Collagen-induced arthritis (CIA) was induced in DBA/1J mice as previously described [14,15]. Briefly, 2 mg/ml chicken type II collagen (CO II) (Sigma) and complete Freund's adjuvant solution (1:1) (RD)was slowly inject a 200 μl volume intradermally into the tail, and a secondary immunization is performed after 21 days of primary injection. PBS treated mice were used as control.

Apigenin (Sigma) was administered intraperitoneally (20 mg/kg bodyweight) one day before the first collagen injection, with treatment continued daily for 50 days [13]. The mice were carefully monitored for the development and severity of joint inflammation, and scored by using an established semi-quantitative scoring system of 0–4 where 0 = normal, 1 = mild swelling, 2 = moderate swelling, 3 = swelling of all joints and 4 = joint distortion and/or rigidity and dysfunction [16].

2.3. H&E staining

Frozen sections were prepared from the joints of the mice, and stained with haematoxylin and eosin, and the score blinded for signs of arthritis.

2.4. Immunohistochemistry

Paraffin sections of the joints or FLS were fixed and stained with antibodies against VEGF, VEGFR1, VEGFR2, RANKL, RANK, OPG, CD68, (Abcam) Vimentin (proteintech) or anti-goat IgG in 4 °C for overnight. After washing with PBS, biotin-labeled anti-goat IgG secondary antibody was incubated for 45 min at 37 °C. The visualization signal was developed with 3,3′-diaminobenzidine tetrachloride (RD). The images were obtained to analyze the Integrated Optical Density (IOD).

2.5. Western blot analysis

Synovial tissues were homogenized and lysed in NETN buffer (20 mM Tris-HCl pH 7.4, 0.5% NP40, 420 mM NaCl, 1 mM EDTA, 1 mM PMSF, 10 μg/ml aprotinin and 10 μg/ml leupeptin) with sonication at 4 °C for 60 min. The supernatants were collected for Western blot analysis, and protein concentration was determined by the Folin assay. Equal amounts protein samples were run in SDS-PAGE and transbolting to PVDF membranes. Antibodies against VEGF (1:500), VEGFR1 (1:1000), VEGFR2 (1:1000), RANKL (1:500), RANK (1:1000), OPG (1:500), β-actin (1:1000) and horseradish perosidase (HRP)-conjugated secondary antibody (1:5000) were used, and the specific protein levels were visualized by using ECL as the HRP substrate. The densitometry of each band was measured by Quantity One 1-D Analysis Software (Bio-Rad). β-actin was used as an internal control for quantification.

2.6. qRT-PCR

RNA purified from synovial tissues by TRIzol Reagent (Invitrogen). Various genes expressions were examined by qRT-PCR using SYBR green real-time PCR Master Mix (TOYOBO). *Actb* was quantified as internal control. The primers used are described in Table 1.

2.7. Isolation and culture of fibroblast-like synoviocytes (FLS)

FLS was purified from control and CIA mice as previous our report [17], and cultured in DMEM medium (Gibco, Grand Island, NY, USA) supplemented with 15% fetal calf serum, 2 mM glutamine (Gibco), penicillin (100 U/ml) and streptomycin (100 μg/ml), and maintained at 37 °C with CO_2 in a humidified atmosphere. Briefly, 8-12pieces (1 mm^3) synovial tissues were evenly placed on the bottom of a culture bottle and culture for 24 h. Then the synovial pieces were removed and continue to culture until 70–80% confluence for passage and amplification in DMEM medium without API. API was added to FLS from CIA mice at indicated concentration for indicated time.

2.8. MTT analysis

FLSs were seeded into 96-well plates and incubated overnight. FLSs were treated with or without API (15, 25, 50, 75, 100, 150, 200 μM) for 24, 48, 72 and 96 h and then collected for MTT analysis as previously [18]. Cells were washed three times by PBS and incubated in 100 μl of 0.5 mg/ml MTT solution at 37 °C for 3 h. The residual cell layer was dissolved in 150 μl of DMSO, the optical density was measured at 490 nm wavelength using a microplate reader (Thermo Scientific, Shanghai, China). Inhibition ratio was calculated.

2.9. Flow cytometric analysis

FLSs were treated with or without 15, 25 and 50 μM API for 24 h. Apoptosis cells were labeled by Annexin V-FITC Apoptosis Detection Kit (Beyotime, C1062S). For cell cycle analysis, FLSs was fix in 70% EtOH at 4 degree for overnight. PI was used for DNA straining with RNase A. After washing, the cells were scraped and suspended in PBS, and 10,000 cells were analyzed by a FACScan flow cytometer (Becton Dickinson, Franklin Lakes, NJ, USA).

2.10. Statistical analysis

Analyses were performed using SPSS 21.0. Data are presented as mean ± standard deviation (SD). The difference of means among

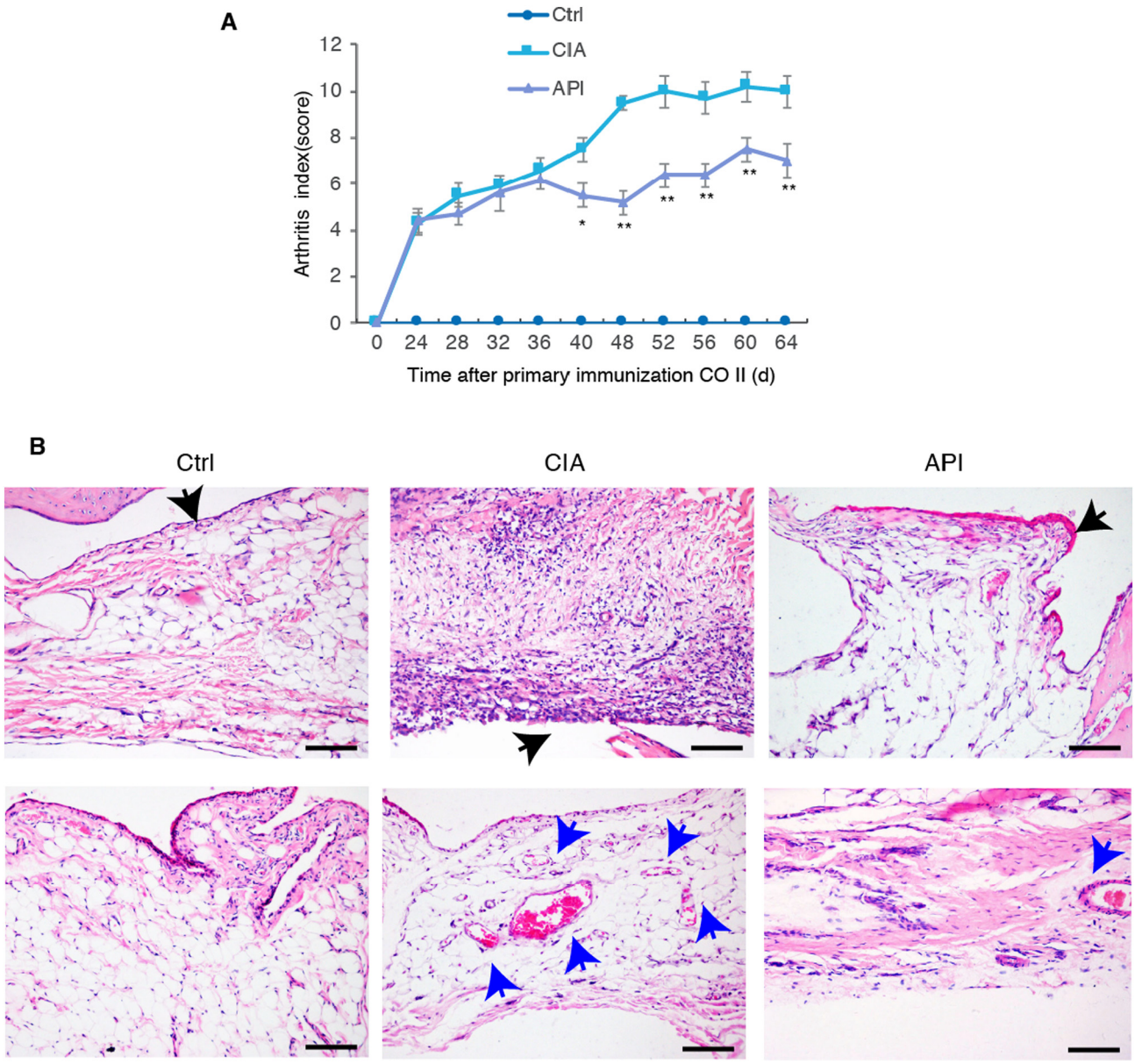

Fig. 1. API inhibits arthritic symptoms in CIA mice. (**A**) Arthritis index was measured between day 24 and day 64 after the first CO II or PBS treatment. PBS (Ctrl), CO II (CIA), and API (API) were administered as described in the Materials and methods section. Data are expressed as mean ± SD, n = 10, *p < 0.05, **p < 0.01. (B) Representative HE staining images of synovial tissues from control, CIA, and API-treated CIA mice on day 48. Synovial hyperplasia (black arrows) and pannus (blue arrows) are marked. (For interpretation of the references to color in this figure legend, the reader is referred to the web version of this article.)

groups were compared by one-way analysis of variance (ANOVA) followed by post hoc LSD (least significant difference) tests.

3. Results

3.1. API inhibits arthritis symptoms in CIA mice

A CIA mouse model, the most commonly studied autoimmune model of RA, was used for the analysis of API function. In CIA mice, arthritic symptoms were observed on day 24 and the arthritic index (AI) representing the severity of RA rapidly increased over time and reached a peak on day 48. The addition of API significantly repressed the CIA-induced increase of the AI score on day 40 (Fig. 1A). This indicated that API could inhibit the arthritic symptoms of RA. Furthermore, joint histomorphological studies indicated that the API addition reduced the CIA-induced increase of synovial hyperplasia, inflammatory cell infiltration, dilatation, and congestion in blood vessels and pannus (Fig. 1B). This indicated that API could inhibit the arthritic symptoms by repressing the synovial hyperplasia, angiogenesis, and osteoclast activation.

3.2. API inhibits FLS proliferation and induces FLS apoptosis in CIA mice

FLSs were isolated from synovial tissue and identified by immunohistochemistry. Vimentin-positive and CD68-negative signals were detected, confirming that the cells were indeed FLSs (Fig. 2A). The cell growth curves were measured to clarify the role of API in FLS proliferation. API treatment significantly repressed the FLS proliferation in a time and dose-dependent manner (Fig. 2B). FACS analysis was also used to analyze cell cycle progression (Fig. 2C) and apoptotic cell percentage (Fig. 2D). In CIA mouse FLSs, G2/S phase was increased and G1 phase was decreased, indicating that cell proliferation was enhanced. After the API addition, G1 phase cell number was significantly increased and G2/S phase cell number was significantly decreased in a

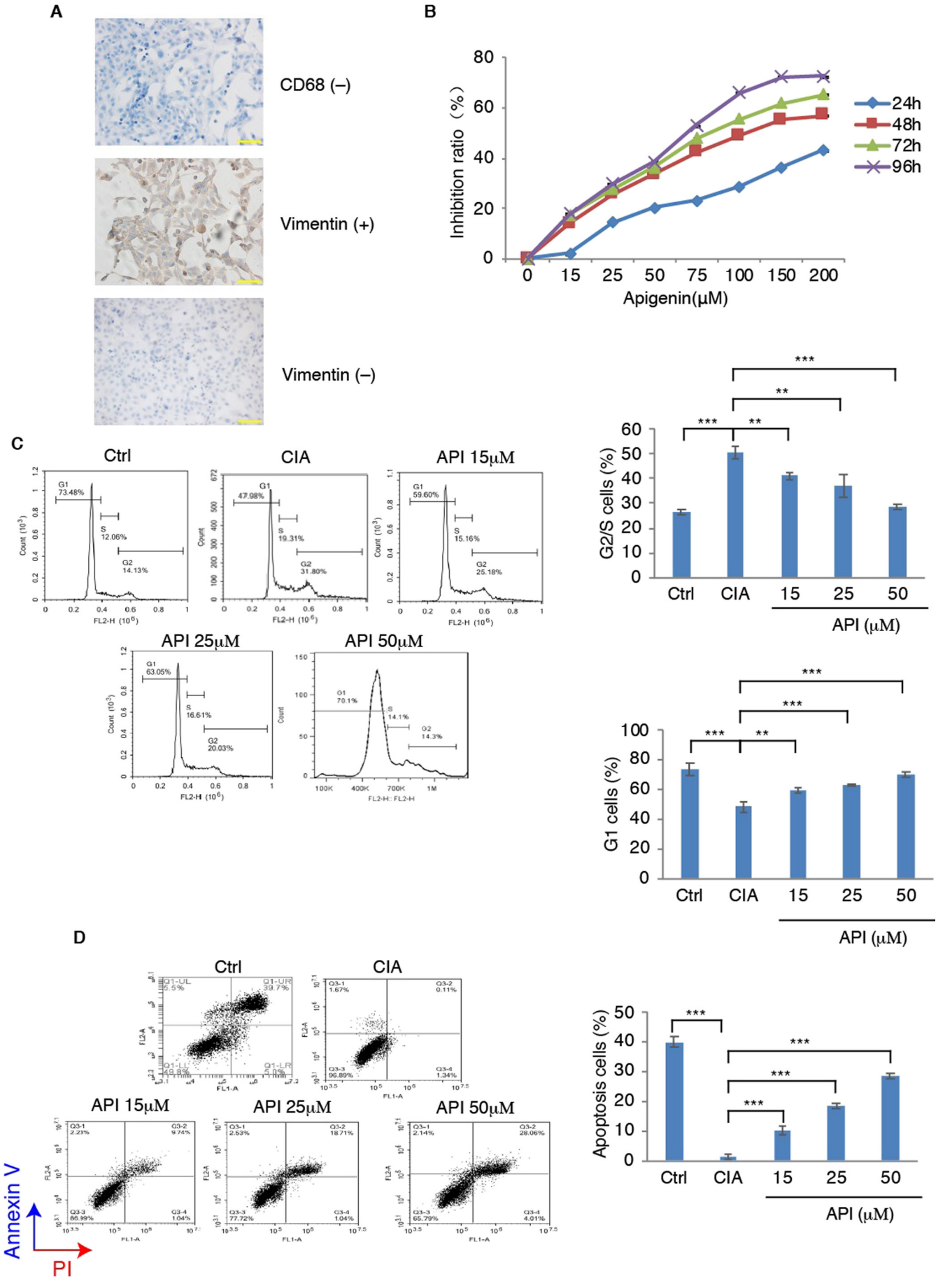

(caption on next page)

Fig. 2. API induces FLS apoptosis and cell cycle arrest. (A) Representative FLS immunostaining images for CD68 and vimentin. CD68-negative and vimentin-positive cells were observed among the FLSs. Vimentin-negative control was stained without antibody. (B) The inhibition ratio of API on FLS was measured by MTT assay. FLSs form CIA mice was treated with or without 15, 25, 50, 75, 100, 150, and 200 μM API for 24, 48, 72, and 96 h. Data are expressed as mean ± SD, n = 3. (C) API induced G2/S cell arrest in FLSs. Cell cycle was measured by FACS with PI staining. FLSs from CIA mice were treated with 15, 25, and 50 μM API for 48 h. The percentages of FLSs in G1 and G2/S phases are shown as mean ± SD, n = 4, **p < 0.01, ***p < 0.001. (D) API-induced increased FLS apoptosis was measured by FACS with Annexin V and PI staining. FLSs from CIA mice were treated with 15, 25, and 50 μM API for 48 h. AV-positive and PI-positive cells represented the apoptotic cells. Apoptotic cell percentages are shown as mean ± SD, n = 4, ***p < 0.001.

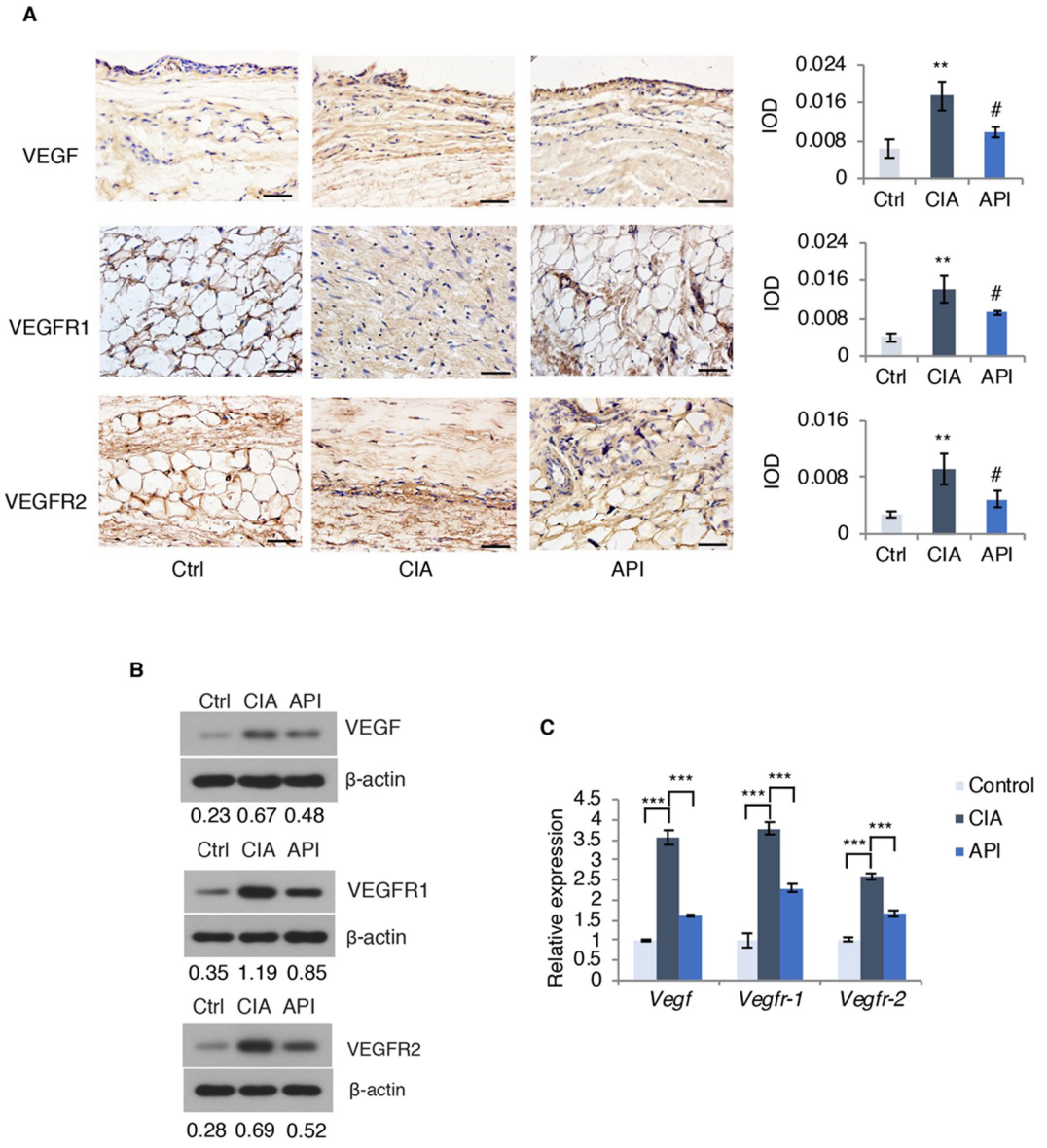

Fig. 3. API represses VEGF and VEGFR expression in synovial tissues of CIA mice. (A) Representative IHC staining images for VEGF, VEGFR-1, and VEGFR-2 in mouse synovial tissue on day 48. PBS (Ctrl), CO II (CIA), and API (API) were administered as described in the Materials and methods section. Integrated optical density (IOD) representing the expression levels was measured. Data are expressed as mean ± SD, n = 3, **p < 0.01 vs. Ctrl group, # p < 0.05 vs. CIA group. (B) Western blot was used to measure the protein levels of VEGF, VEGFR-1, and VEGFR-2 in synovial tissues from control, CIA, and API mice on day 48. The relative densitometry ratios to β-actin are shown below. (C) mRNA levels of *Vegf*, *Vegfr-1,* and *Vegfr-2* genes were measured by qRT-PCR on day 48. *Actb* was measured as an internal control. The relative expression levels are shown as mean ± SD, n = 4, ***p < 0.001.

dose-dependent manner (Fig. 2C). This suggested that API slowed cell cycle progression and thereby inhibited cell proliferation in CIA mice. Moreover, Annexin V (AV)-PI staining indicated that the late apoptosis cell ratio was significant, since AV-positive and PI-positive cell proportion was around 40% in control mice. CIA significantly repressed the apoptotic cell numbers, while the apoptotic cell percentage was significantly increased after the API treatment in a dose-dependent manner (Fig. 2D). Thus, API could rebalance the proliferation and apoptosis status in RA.

3.3. API can inhibit VEGF and VEGFR expression in CIA mice

Potent pro-angiogenic cytokine vascular endothelial growth factor (VEGF) and its receptor VEGFR have been demonstrated to have a central involvement in the angiogenic process and pannus formation in RA [19,20]. Therefore, VEGF and VEGFR expression levels were

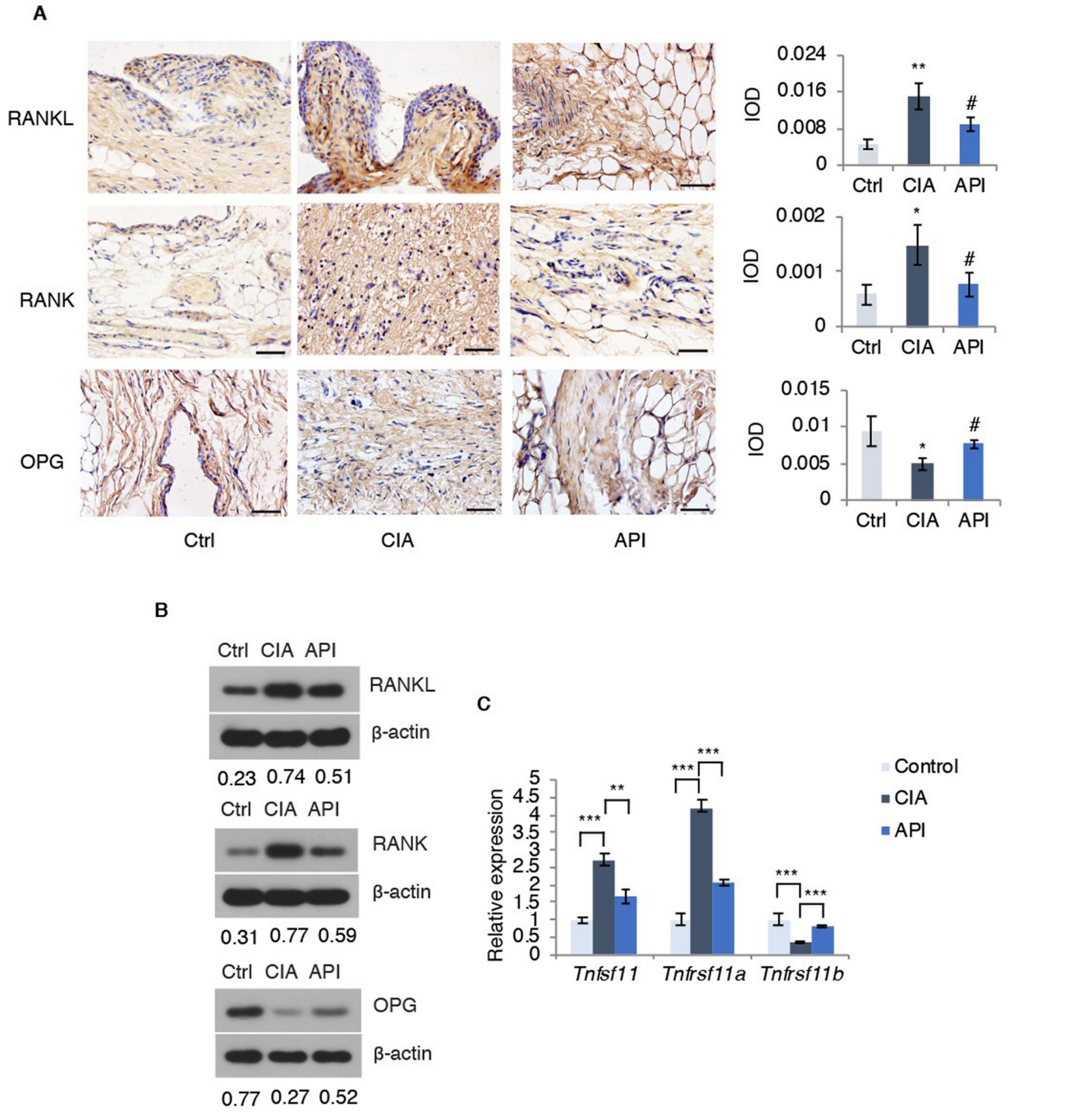

Fig. 4. API regulates RANKL/RANK/OPG system in synovial tissues of CIA mice. (A) Representative IHC staining images for RANKL, RANK, and OPG in synovial tissues from control, CIA, and API mice on day 48. CO II (CIA) and API (API) were administered as described in the Materials and methods section. IOD representing the expression levels were measured. Data are expressed as mean ± SD, n = 3, *p < 0.05, **p < 0.01 vs. Ctrl group, #p < 0.05 vs. CIA group. (B) Western blot was used to measure the protein levels of RANKL, RANK, and OPG in synovial tissues from control, CIA, and API mice on day 48. The relative densitometry ratios to β-actin are shown below. (**C**) mRNA levels of *Tnfsf11, Tnfrsf11a,* and *Tnfrsf11b* genes were measured by qRT-PCR on day 48. *Actb* was measured as an internal control. The relative expression levels are shown as mean ± SD, n = 4, **p < 0.01, ***p < 0.001.

analyzed by IHC (Fig. 3A) and western blot (Fig. 3B). Both IHC and western blot results indicated higher levels of VEGF, VEGFR 1, and VEGFR 2 expression in synovial tissues of CIA mice. API significantly decreased the protein levels of VEGF, VEGF1, and VEGFR2. The mRNA levels were measured by qRT-PCR (Fig. 3C). Similar results were observed, where API repressed the *Vegf*, *Vegf1,* and *Vegf2* gene transcription in CIA mice. Thus, it was suggested that API could repress VEGF and VEGFR expression in RA.

3.4. API regulates RANKL/RANK/OPG system in CIA mice

The RANKL/RANK/OPG system plays a key role in osteoclastogenesis. RANKL binds to the RANK receptor on osteoclast precursors and subsequently drives osteoclastogenesis, while osteoprotegerin (OPG) in osteoblasts acts as a decoy receptor for RANKL, which prevents RANKL binding to RANK [21,22]. Therefore, we analyzed the RANKL/RANK/OPG system in API-treated CIA mice. IHC and western blot results indicated that RANKL and RANK expression levels were significantly reduced after the API treatment in CIA mice. The expression of OPG was

significantly increased in API-treated CIA mice (Fig. 4A, B). RT-PCR was used to quantify the mRNA levels of *Tnfsf11, Tnfrsf11a,* and *Tnfrsf11b* encoding RANKL, RANK, and OPG, respectively. Decreased *Tnfsf11 and Tnfrsf11a*, and increased *Tnfrsf11b* expression levels were observed in API-treated groups in CIA mice. This suggested that API repressed osteoclastogenesis via the RANKL/RANK/OPG system in RA.

4. Discussion

In RA, imbalance between FLS proliferation and apoptosis has been regarded as a contributing factor for the development of RA, since excessive growth of the FLSs promotes hyperplasia of synovial tissues and induces its invasion into the bone and cartilage, eventually leading to joint deformity and dysfunction [3,23]. However, FLSs in RA rarely undergo apoptosis (< 2% in CIA mice, Fig. 2D), since high levels of Bcl-2 expression might block the mitochondria/caspase apoptosis pathway in the RA joints [24]. Here, API was found to promote apoptosis and induce G2/S phase cell cycle arrest in cultured FLSs, since API exerts transient effect in CIA mice (daily administration) and the long time FLSs isolation and culture process in DMEM without API might omit the pro-apoptosis function of FLSs. Furthermore, API was reported to induce the mitochondrial redox impairment and increased mitochondria reactive oxygen species (ROS) levels in human cervical cancer-derived cell lines [25]. The mitochondria/caspase pathway was also reported to participate in API-induced cell apoptosis in human breast cancer [26]. Thus, API inhibition of FLS growth and synovial hyperplasia in RA might occur through regulation of ROS and mitochondria/caspase pathway in RA.

API inhibits VEGF and VEGFR, which might contribute to anti-angiogenesis in RA, since VEGF is the most endothelial-cell-specific factor and induces vascular permeability. Serum VEGF was elevated in RA and correlated with the radiographic progression of vascularity over the subsequent year. [4] VEGFR-1 and VEGFR-2 are closely related receptor tyrosine kinases and are required for normal development and angiogenesis [27]. Deletion of the tyrosine kinase domain of VEGFR-1 decreases the incidence and clinical symptoms of RA, such as inflammatory infiltration, while the pannus formation becomes milder in *Vegfr-1* mutant mice [28]. On the other hand, API suppresses the expression of VEGF via degradation of hypoxia-inducible factor (HIF)-1α protein in endothelial cells and human lung cancer cells [29,30]. Interestingly, HIF-1α is a key transcriptional factor that is highly expressed in the RA synovium to regulate the adaptive responses to this hypoxic environment. Both HIF-1α and HIF-2α have been shown to increase the expression of VEGF in the inflammatory joint region and to further induce angiogenesis [31,32]. Thus, the anti-angiogenic activity of API might occur via the HIF-1α/VEGF pathway in RA.

The RANKL/RANK/OPG system is a well understood signaling pathway that contributes to osteoclastogenesis and bone destruction in RA. In postoperative joint specimens of patients with RA, increased number of osteoclasts and RANKL expression levels were found [33]. Therefore, API could repress and delay in the osteoclastogenesis process in RA by regulating the RANKL/RANK/OPG system. Moreover, the expression of RANKL/RANK/OPG is mainly regulated by hormones, growth factors, and cytokines, including IL-1, IL-6, IL-11, IL-17, and TNFα [34]. In mouse osteoblast cells, API inhibits the osteoclastogenic cytokines, IL-6 RANTES, MCP-1, and MCP-3 in a dose-dependent manner, further repressing the RANKL expression [35]. This suggests that API might regulate the expression of the RANKL/RANK/OPG system by regulating various cytokines. Here, inflammatory cell infiltration was repressed after the API treatment (Fig. 1A), which partly indicated that API regulates the RANKL/RANK/OPG system via some inflammatory cytokines in RA. Furthermore, API was also reported to target the RANKL/RANK/OPG system in in silico research [36]. Based on the three-dimensional structure models of RCSB RANK-RANKL and RANKL-OPG, API easily interacts with the RANK-RANKL and RANKL-OPG systems. Thus, the anti-osteoclastogenesis activity of API might act by not only changing the expression of the RANKL/RANK/OPG system but also regulating the interaction of RANK-RANKL and RANKL-OPG in RA.α.

The majority functions of flavones result from their strong anti-oxidative properties, API was therefore thought to scavenge mitochondria ROS, which regulates numerous intracellular signal transduction pathways as well as the activities of various transcription factors [37,38]. Increased ROS level has been reported to active HIF-1α/VEGF pathway and contribute to angiogenesis [39] and regulate osteoclastogenic cytokines expression and mediate RANK signaling [40]. Moreover, inflammatory cytokines, such as IL-6, TNF-α, in the synovium of RA patients could be augmented by the generation of ROS in the FLSs, since *N*-acetylcysteine, ROS scavenger, inhibited the IL-6 and TNF-α in FLSs [41]. And ROSs and inflammatory cytokines were found to be elevated in RA patients in comparison with the healthy controls [42]. Therefore, the multi-functions of API might be due to the antioxidative properties. But API has been reported to induce ROS and apoptosis in cancer cell lines [25]. The complex and controversial role of API in ROS generation might be because different subtypes ROS were regulated by API in different directions [43]. Thus, the multi-functions of API in RA could be due to a common molecular target mitochondria ROS.

Thus, API might repress the pathogenesis process of RA to improve the arthritic symptoms by inhibiting synovial hyperplasia, angiogenesis, and osteoclastogenesis. API-induced decreased FLS proliferation and increased FLS apoptosis could act against synovial hyperplasia, the anti- angiogenesis function of API might inhibit VEGF and VEGFR expression, while its anti-osteoclastogenesis activity can regulate the RANKL/RANK/OPG system. Therefore, API might be a putative low toxicity candidate drug for RA treatment.

Declaration of Competing Interest

The authors declare no conflicts of interest regarding the content herein.

Acknowledgements

This work was supported by the Natural Science Foundation of Liaoning Province (Grant no. 20170540865) and Clinical Science and Technology Fund of Shenyang Medical College (Grant no. 20181002).

References

[1] E.D. Harris, Rheumatoid arthritis: pathophysiology and implications for therapy, N. Engl. J. Med. 322 (1990) 1277–1289.
[2] B. Bartok, G.S. Firestein, Fibroblast-like synoviocytes: key effector cells in rheumatoid arthritis, Immunol. Rev. 233 (2010) 233–255.
[3] H. Li, A. Wan, Apoptosis of rheumatoid arthritis fibroblast-like synoviocytes: possible roles of nitric oxide and the thioredoxin 1, Mediat. Inflamm. 2013 (2013) 953462.
[4] E.M. Paleolog, Angiogenesis in rheumatoid arthritis, Arthritis Res. 4 (3) (2002) S81–S90.
[5] G. Schett, Cells of the synovium in rheumatoid arthritis, Osteoclasts. Arthritis Res Ther 9 (2007) 203.
[6] Y. Shigeyama, T. Pap, P. Kunzler, B.R. Simmen, R.E. Gay, S. Gay, Expression of osteoclast differentiation factor in rheumatoid arthritis, Arthritis Rheum. 43 (2000) 2523–2530.
[7] Y. Tanaka, Clinical immunity in bone and joints, J. Bone Miner. Metab. 37 (2019) 2–8.
[8] P. Geusens, The role of RANK ligand/osteoprotegerin in rheumatoid arthritis, Ther Adv Musculoskelet Dis 4 (2012) 225–233.
[9] K.L. Soeken, S.A. Miller, E. Ernst, Herbal medicines for the treatment of rheumatoid arthritis: a systematic review, Rheumatology (Oxford) 42 (2003) 652–659.
[10] S. Shukla, S. Gupta, Apigenin: a promising molecule for Cancer prevention, Pharm. Res. 27 (2010) 962–978.
[11] H.K. Kang, D. Ecklund, M. Liu, S.K. Datta, Apigenin, a non-mutagenic dietary flavonoid, suppresses lupus by inhibiting autoantigen presentation for expansion of autoreactive Th1 and Th17 cells, Arthritis Res Ther 11 (2009) R59.
[12] J. Li, B. Zhang, Apigenin protects ovalbumin-induced asthma through the regulation of Th17 cells, Fitoterapia 91 (2013) 298–304.
[13] X. Li, Y. Han, Q. Zhou, H. Jie, Y. He, J. Han, et al., Apigenin, a potent suppressor of

dendritic cell maturation and migration, protects against collagen-induced arthritis, J. Cell. Mol. Med. 20 (2016) 170–180.
[14] D.D. Brand, K.A. Latham, E.F. Rosloniec, Collagen-induced arthritis, Nat. Protoc. 2 (2007) 1269–1275.
[15] Y. Li, S. Wu, Y. Li, S. Jiang, T. Lin, L. Xia, H. Shen, J. Lu, Interleukin-35 (IL-35) inhibits proliferation and promotes apoptosis of fibroblast-like synoviocytes isolated from mice with collagen-induced arthritis, Mol. Biol. Rep. 43 (2016) 947–956.
[16] S. Sarkar, L.A. Cooney, P. White, D.B. Dunlop, J. Endres, J.M. Jorns, et al., Regulation of pathogenic IL-17A responses in collagen-induced arthritis: roles of endogenous interferon-gamma and IL-4, Arthritis Res Ther 11 (2009) R158.
[17] Y. Li, D. Li, Y. Li, S. Wu, S. Jiang, T. Lin, et al., Interleukin-35 upregulates OPG and inhibits RANKL in mice with collagen- induced arthritis and fibroblast-like synoviocytes, Osteoporos. Int. 27 (2016) 1537–1546.
[18] B. Liu, P. Yang, Y. Ye, Y. Zhou, L. Li, S. Tashiro, S. Onodera, T. Ikejima, Role of ROS in the protective effect of silibinin on sodium nitroprusside-induced apoptosis in rat pheochromocytoma PC12 cells, Free Radic. Res. 45 (2011) 835–847.
[19] P.C. Taylor, VEGF and imaging of vessels in rheumatoid arthritis, Arthritis Res. 4 (Suppl. 3) (2002) S99–107.
[20] A.O. Afuwape, S. Kiriakidis, E.M. Paleolog, The role of the angiogenic molecule VEGF in the pathogenesis of rheumatoid arthritis, Histol. Histopathol. 17 (2002) 961–972.
[21] Á. Szentpétery, Á. Horváth, K. Gulyás, Z. Pethö, H.P. Bhattoa, S. Szántó, G. Szücs, O. FitzGerald, G. Schett, Z. Szekanecz, Effects of targeted therapies on the bone in arthritides, Autoimmun. Rev. 16 (2017) 313–320.
[22] D.L. Lacey, E. Timms, H.L. Tan, M.J. Kelley, C.R. Dunstan, T. Burgess, et al., Osteoprotegerin ligand is a cytokine that regulates osteoclast differentiation and activation, Cell 93 (1998) 165–176.
[23] M. Peng, L. Qiang, Y. Xu, C. Li, T. Li, J. Wang, IL-35 ameliorates collagen-induced arthritis by promoting TNF-α-induced apoptosis of synovial fibroblasts and stimulating M2 macrophages polarization, FEBS J. (2019), https://doi.org/10.1111/febs.14801.
[24] A. Kawakami, T. Nakashima, H. Sakai, A. Hida, S. Urayama, S. Yamasaki, H. Nakamura, et al., Regulation of synovial cell apoptosis by proteasome inhibitor, Arthritis Rheum. 42 (1999) 2440–2448.
[25] R.P. Souza, P.S. Bonfim-Mendonça, F. Gimenes, B.A. Ratti, V. Kaplum, M.L. Bruschi, et al., Oxidative stress triggered by apigenin induces apoptosis in a comprehensive panel of human cervical cancer-derived cell lines, Oxidative Med. Cell. Longev. 2017 (2017) 1512745.
[26] E.J. Choi, G.H. Kim, Apigenin induces apoptosis through a mitochondria/caspase-pathway in human breast cancer MDA-MB-453 cells, J. Clin. Biochem. Nutr. 44 (2009) 260–265.
[27] N. Rahimi, VEGFR-1 and VEGFR-2: two non-identical twins with a unique physiognomy, Front. Biosci. 11 (2006) 818–829.
[28] M. Murakami, S. Iwai, S. Hiratsuka, M. Yamauchi, K. Nakamura, Y. Iwakura, M. Shibuya, Signaling of vascular endothelial growth factor receptor-1 tyrosine kinase promotes rheumatoid arthritis through activation of monocytes/macrophages, Blood 108 (2006) 1849–1856.
[29] M. Osada, S. Imaoka, Y. Funae, Apigenin suppresses the expression of VEGF, an important factor for angiogenesis, in endothelial cells via degradation of HIF-1alpha protein, FEBS Lett. 575 (2004) 59–63.
[30] I.J. MacDonald, S.C. Liu, C.M. Su, Y.H. Wang, C.H. Tsai, C.H. Tang, Implications of angiogenesis involvement in arthritis, Int. J. Mol. Sci. 19 (2018) (pii: E2012).
[31] S. Hua, T.H. Dias, Hypoxia-inducible factor (HIF) as a target for novel therapies in rheumatoid arthritis, Front. Pharmacol. 7 (2016) 184.
[32] H.A. Elshabrawy, Z. Chen, M.V. Volin, S. Ravella, S. Virupannavar, S. Shahrara, The pathogenic role of angiogenesis in rheumatoid arthritis, Angiogenesis 18 (2015) 433–448.
[33] N. Dalbeth, T. Smith, S. Gray, A. Doyle, P. Antill, M. Lobo, et al., Cellular characterisation of magnetic resonance imaging bone oedema in rheumatoid arthritis; implications for pathogenesis of erosive disease, Ann. Rheum. Dis. 68 (2009) 279–282.
[34] L.E. Theill, W.J. Boyle, J.M. Penninger, RANK-L and RANK: T cells, bone loss, and mammalian evolution, Annu. Rev. Immunol. 20 (2002) 795–823.
[35] S. Bandyopadhyay, J.M. Lion, R. Mentaverri, D.A. Ricupero, S. Kamel, J.R. Romero, et al., Attenuation of osteoclastogenesis and osteoclast function by apigenin, Biochem. Pharmacol. 72 (2006) 184–197.
[36] Z. Noor, N. Kania, A. Azharuddin, N. Budhiparama, N. Nurdiana, N.N. Hidajat, et al., The interaction of the active compounds of Labisia pumila on RANKeRANKLeOPG system, Clinical Nutrition Experimental 17 (2018) 23–27.
[37] C. Brunetti, M. Di Ferdinando, A. Fini, S. Pollastri, M. Tattini, Flavonoids as antioxidants and developmental regulators: relative significance in plants and humans, Int. J. Mol. Sci. 14 (2013) 3540–3555.
[38] S. Das, J. Das, A. Paul, A. Samadder, A.R. Khuda-Bukhsh, Apigenin, a bioactive flavonoid from Lycopodium clavatum, stimulates nucleotide excision repair genes to protect skin keratinocytes from ultraviolet B-induced reactive oxygen species and DNA damage, J Acupunct Meridian Stud 6 (2013) 252–262.
[39] M. Ushio-Fukai, Y. Nakamura, Reactive oxygen species and angiogenesis: NADPH oxidase as target for cancer therapy, Cancer Lett. 266 (2008) 37–52.
[40] H. Ha, H.B. Kwak, S.W. Lee, H.M. Jin, H.M. Kim, H.H. Kim, Z.H. Lee, Reactive oxygen species mediate RANK signaling in osteoclasts, Exp. Cell Res. 301 (2004) 119–127.
[41] J.Y. Sung, J.H. Hong, H.S. Kang, I. Choi, S.D. Lim, J.K. Lee, J.H. Seok, J.H. Lee, G.M. Hur, Methotrexate suppresses the interleukin-6 induced generation of reactive oxygen species in the synoviocytes of rheumatoid arthritis, Immunopharmacology 47 (2000) 35–44.
[42] S. Mateen, S. Moin, S. Shahzad, A.Q. Khan, Level of inflammatory cytokines in rheumatoid arthritis patients: correlation with 25-hydroxy vitamin D and reactive oxygen species, PLoS One 12 (2017) e0178879.
[43] G. Bartosz, Reactive oxygen species: destroyers or messengers, Biochem. Pharmacol. 77 (2009) 1303–1315.